Article:
Esfahani, M N, Jabbari, M, Xu, Y et al. (2021) Effect of nanoscale defects on the thermal conductivity of graphene. Materials Today Communications, 26. 101856. ISSN: 2352-4928

https://doi.org/10.1016/j.mtcomm.2020.101856

Effect of Nanoscale Defects on the Thermal Conductivity of Graphene

Mohammad Nasr Esfahani[a,*], Masoud Jabbari[b], Yongbing Xu[a], Costas Soutis[c]

[a] *Department of Electronic Engineering, University of York, York YO10 5DD, UK*
[b] *Department of Mechanical, Aerospace and Civil Engineering, University of Manchester, Manchester M13 9PL, UK*
[c] *Aerospace Research Institute, University of Manchester, Manchester, Manchester M13 9PL, UK*

Abstract

There are remarkable theoretical efforts geared towards understanding the impact of fabrication-induced defects on the operational behaviour of a single layer graphene. These studies have been focused mainly on atomic defects, while nanoscale pinholes and patches of two layers thick (bilayer) attached on a monolayer graphene are inevitable during the synthesis process. In this work the influence of these nanoscale defects on the graphene thermal conductivity is studied via non-equilibrium molecular dynamics simulations. The thermal conductivity of a single layer zigzag and armchair oriented graphene is modelled capturing the effect of voids and bilayer imperfections. A single layer graphene sheet with a size of 50 nm $\times$ 10 nm is analysed having an elliptical defect of up to 6 nm (major axis). Our results exhibit a reduction of over 20 % in thermal conductivity with increasing temperature and about 75 % drop with increasing void size. The decrease in the thermal conductivity is 15 % for the single layer graphene with a bilayer defect of 6 nm in diameter. This study demonstrates a dramatic influence of defect shape on the thermal conductivity of graphene, where defects with elliptical shapes demonstrate a higher thermal transfer in graphene compared to circular ones. This work provides a guideline of how to quantify the effect of fabrication induced defects on thermal conductivity of graphene.

Keywords: Graphene, Thermal Conductivity, Pinhole, Bilayer, Molecular Dynamics

1. Introduction

Graphene – as a 2D sheet of carbon atoms arranged in a honeycomb lattice – has introduced unique properties with a wide range of applications in bioengineering [1], electronics [2], energy storage [3] and composite structures [4–6]. In addition to superior electrical conductivity and mechanical strength [7, 8], an outstanding thermal conductivity has been reported for the single layer graphene [9, 10]. This raises attentions to use graphene for multi-functional purposes. For example, graphene is utilised in batteries as an electrode to enhance device performance as well as thermal management applications [11, 12]. Although the extreme thermal conductivity of graphene can be obtained for the perfect crystal structure without defects [9, 10, 13], porosities in graphene — as an electrode — improve ions and electrons transports in energy storage devices [14]. Furthermore, defects are inevitable during the synthesis and integration processes [15–17], which have profound influence on the thermal conductivity of graphene. This has inspired many studies to understand the thermal behaviour of defective graphene-based structures.

Experimental measurements have demonstrated a wide range of thermal conductivity for the single layer graphene [9, 10, 18], which is attributed to various parameters including substrate, size and defects [13, 19]. Those defects mainly include point vacancies, impurities, and dislocations [15, 20]. In addition to those atomic scale defects, nanoscale pinholes and multi-layer regions are other imperfections, which can be imposed during the manufacturing processes [16, 21–24]. Those defects can be induced intentionally as well

*Corresponding author
Email address: mohammad.nasresfahani@york.ac.uk (Mohammad Nasr Esfahani)

for nanoengineering purposes. For example, nanoporous graphene has offered numerous applications in the field of sensing and energy storage [12, 14, 25]. Therefore, taking into account the influence of defects on the thermal conductivity of graphene has become the motivation of various studies. Experimental observations report a dramatic decrease in the thermal conductivity of defective graphene [26]. To support experimental studies, theoretical approaches have been used widely to understand the impact of defects on the thermal behaviour. Molecular dynamics (MD) simulations are found to be a useful tool among various theoretical techniques to model the thermal conductivity of graphene [27–29].

A series of studies has employed MD simulations to understand the thermal transfer in graphene with various defects. This includes vacancies [27, 30], Stone-Wales (SW) [31, 32] and nitrogen doping [33] defects, which generally reduce the thermal conductivity of graphene with different intensities. In addition to those crystal imperfections, recent studies focus on the effect of voids on the thermal behaviour of graphene [34]. Although those works have examined the thermal conductivity of graphene with atomic imperfections, scale effect is the primary challenge to understand the physical behaviour of nanostructures [35]. A high density nanoscale pinhole defects with a wide range of diameters of 1 nm to 10 nm has been observed during the graphene synthesis processes [21]. Moreover, few-layer regions form during the fabrication monolayer graphene — especially in epitaxial processes — with significant impacts on the physical behaviour through structural non-uniformity [16, 36, 37]. For example, thermal annealing the substrate during epitaxial processes can initiate a new graphene layer before a complete formation of the first layer on the entire surface [16, 38]. Step edges on the substrate is another reason to create bilayer regions in single layer graphene sheets [36]. Moreover, a non-uniform exfoliation process leaves bilayer defects in monolayer graphene [16, 39]. While atomic-scale defects have been the centre of attention for most of theoretical works so far [27, 30–34], the effect of those nanosale defects on the graphene thermal transport necessitates to be addressed to bridge the gap between atomic and micro-scale defects. This work uses atomic simulations to understand the effect of nanoscale pinholes (voids) and bilayer regions on the thermal conductivity of the single layer graphene. Non-equilibrium MD (NEMD) method is carried out along the zigzag and armchair orientations of graphene sheets at the temperature in a range of 100 K to 500 K. This study will present the theoretical framework of the NEMD method. Then, void and bilayer defects will be studied focusing on the size effect on the thermal transport. After comparing with atomic scale defects, this study will be concluded with a discussion on the effect of void and bilayer shape on the thermal behaviour of graphene.

2. Simulation Methods

This work employs MD simulations to study the effect of voids and bilayer defects on the thermal conductivity of graphene. The optimized Tersoff potential [40] is used in LAMMPS code [41] to model the thermal transport along zigzag and armchair directions. Graphene sheets with size of 50 nm $\times$ 10 nm are considered with circle shape defects (void or bilayer region) at the centre in a diameter of D as shown in Fig. 1. Those nanoscale defects can form during the graphene synthesis processes [16, 21, 36]. The considered simulation dimensions are an average graphene sheet size for theoretical studies [31, 42, 43]. Lennard-Jones potential [44] is used to model the interaction between inter-layers in bilayer defects (inset in Fig.1 (b)). Periodic boundary condition is applied along x- and y-directions to represent graphene sheets rather than graphene nanoribbons. In this study, NEMD method is utilised to measure the thermal conductivity at temperature of 100 K to 500 K, which is the major framework among theoretical simulations on the graphene thermal analysis [27, 30–34]. In this method, carbon atoms at two ends of graphene sheets are fixed to avoid from sublimating (grey shaded atoms in Fig. 1). Then, other atoms are divided into sub-groups along the longitudinal direction (x-direction). The first sub-group is considered as the cold reservoir, while the last sub-group is assigned as the hot reservoir (inset in Fig.1 (a)). All simulations are carried out with a time step of 1 fs. The graphene sheets were first relaxed using canonical (NVT) ensemble by the Nose-Hoover thermostat for 100 ps. This is followed by applying a temperature difference along x-direction. In this step, the temperature of atoms in the cold reservoir is reduced for 10 K, while the temperature of atoms in the hot reservoir is increased for 10 K. This impose a temperature difference of ΔT =20 K between reservoirs through NVT ensemble, where atoms in the remaining sub-groups are maintained under constant energy

(NVE) for 3 ns. This work studies the thermal conductivity of zigzag and armchiar graphene sheets, which have been studied mainly through theoretical investigations [13]

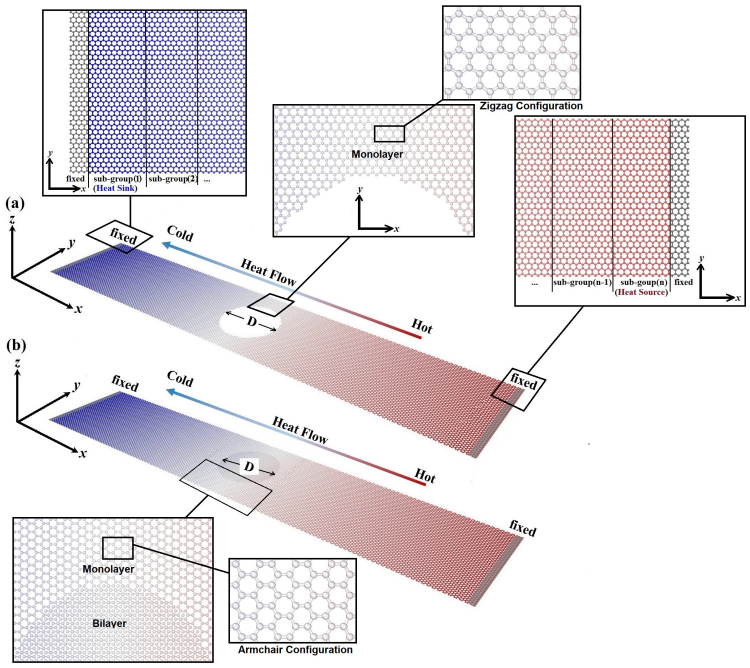

Figure 1: Schematic of NEMD model to evaluate the thermal conductivity of single layer graphene sheets having nanoscale (a) void, and (b) bilayer defects, with a diameter of D. The close-ups in panel (a) demonstrate sub-groups and assigned heat source and heat sink with an inset to void defect in zigzag chirality. The close-up in panel (b) presents bilayer region in monolayer armchair graphene.

To maintain a temperature difference at both ends of graphene sheets in a steady-state condition, the added energy into the hot reservoir should be the same amount as the energy removed from the cold reservoir. The rate of the change of the energy transferred between those sources over time is estimated as the heat flux, q_x. Then, the thermal conductivity, κ, is calculated based on the Fourier law for one-dimensional structures as

$$q_x = -\kappa A_c \frac{dT}{dx} \tag{1}$$

where $\frac{dT}{dx}$ is the temperature gradient and A_c is the cross-sectional area of the structure. Temperature of i^{th} sub-group, T_i, is computed as

$$T_i = \frac{2}{3Nk_B} \sum_j \frac{p_j^2}{2m_j} \tag{2}$$

where p is the momentum, m is atomic mass, N and k_B are number of carbon atoms in this sub-group and the Boltzman constant, respectively. Here the thickness of the single layer graphene is considered as 3.4 $\mathring{A}$ [27, 33]. In the remainder of this work, the thermal conductivity of pristine graphene without any defects is first calculated for temperature of 100 K to 500 K. Then, the influence of defects on the thermal transport will be studied for graphene sheets. This work will be concluded by discussing the effect of void and bilayer shapes on the thermal behaviour of graphene.

3. Results and Discussions

The thermal conductivity of pristine graphene, κ_0, is studied first through using NEMD method. Fig. 2 exhibits the thermal conductivity of defect-free zigzag and armchair graphene sheets at the temperature in a range of 100 K to 500 K compared with previous works [18, 28, 34, 42]. In the first instance, a thermal conductivity in a range of 400 W/Km to 550 W/Km is obtained for defect free graphene sheets, which is comparable the thermal conductivity reported through previous experimental [18] and theoretical studies with the same interatomic potential [28, 34, 42]. The thermal conductivity reduces with increasing temperature for both orientations, while a higher thermal transport is obtained for the zigzag chirality. Although some works predict isotropic thermal conductivity for graphene [45, 46],a higher thermal conductivity in zigzag chirality has been reported for monolayer graphene as well [27, 31–33, 42]. Here, the thermal conductivity of zigzag graphene is found to be 8-20% higher than those armchair sheets, while this anisotropy in the thermal conductivity of graphene nanoribbons can reach to 50% reported in previous studies [27, 32]. This chirality effect is attributed to the phonon scattering rates at the armchair and zigzag edges due to the finite size, where the graphene flake size is less than the phonon mean free path [13, 27]. Similar temperature effect has been reported previously through experimental [9, 13] and computational [13, 33] studies. This reduction in the thermal conductivity can be attributed to the phonon-phonon and phonon-boundary scatterings at higher temperatures [13]. After calculating the thermal conductivity of defect-free graphene, the influence of voids and bilayer defects (Fig. 1) on the thermal transport of graphene sheets is studied through NEMD simulations. In this regard, the heat flux and temperature gradient are analysed to understand the contribution of defects on the thermal behaviour.

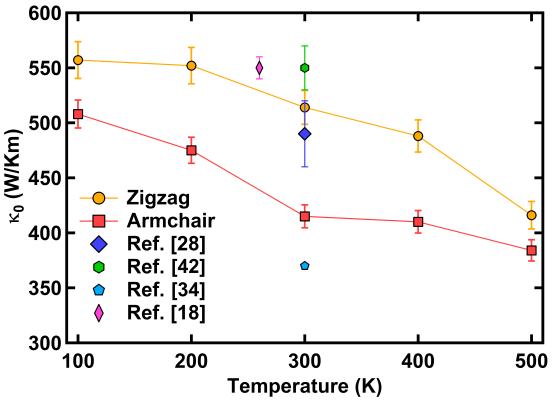

Figure 2: The thermal conductivity of the zigzag and armchair oriented pristine (defect-free) graphene as a function of temperature. To compare with previous studies, results from Ref. [18, 28, 34, 42] are presented.

Fig. 3 shows the amount of energy added to the hot reservoirs and removed from the cold reservoirs of the zigzag graphene sheets with voids and bilayer defects at 100 K. In the first instant, regardless of defects, results exhibit a same energy value exchanged between atoms in the heat source and heat sink regions. The energy exchange has a linear trend over the simulation time, which represents a steady-state heat flux and energy conservation during the simulations. Fig. 3 exhibits a different impact from voids and bilayer defects into the energy exchange of graphene sheets. Although bilayer defects have a negligible effect on the heat flux, increasing the void diameter reduces the amount of energy exchanged between the hot and cold reservoirs. The heat flux changes from 0.77 eV/ps to 0.58 eV/ps with increasing the void diameter from 2 nm to 6 nm. The same effect from voids and bilayer defects on the heat flux was observed for the armchair chirality and higher temperatures.

After calculating the heat flux, the temperature distribution along the longitudinal direction of graphene sheets is estimated for the steady-state condition through using Eq. (2). Fig. 4. demonstrates the temperature profile of the zigzag oriented defective graphene sheets at temperature of 100 K. A part from reservoirs at both ends, the temperature gradient demonstrates a linear trend along the pristine graphene, $(dT/dx)_P$.

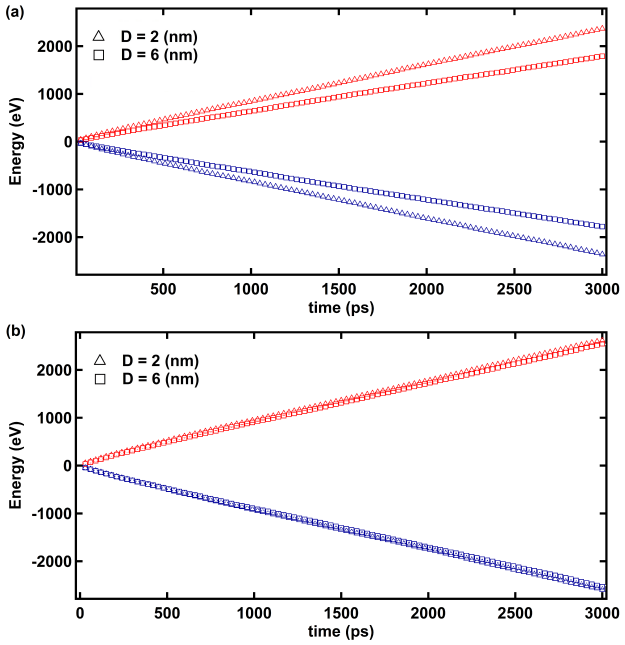

Figure 3: Energy added to hot reservoirs, red marks, and removed from cold reservoirs, blue marks, at a temperature of 100 K for the zigzag graphene sheets having (a) void and (b) bilayer defects with a diameter of D.

Although this linear trend has a higher gradient at the void regions, $(dT/dx)_V > (dT/dx)_P$, the temperature gradient at other locations is the same as the pristine graphene. This implies a different thermal conductivity in slabs at the void position than the groups of atoms without any defect. In contrast, bilayer regions change the temperature gradient along graphene through inducing a spike at the temperature profile.The temperature gradient for defect-free graphene is estimated through fitting linear trend approached following previous works [31–34, 42, 43], while temperature difference divided by the defect length is used to calculate the temperature gradient in defect regions as suggested previously for local nonequilibrium transports [47]. After predicting the temperature gradient and heat flux, the thermal conductivity of defective graphene sheets is calculated as a combination of pristine slabs and a defect region by using the Fourier law in Eq. (1).

Fig. 5 shows the void size effect on the thermal conductivity of graphene at temperature of 100 K to 500 K compared with atomic scale defects [31–33]. The thermal conductivity of defective graphene was normalised by the thermal conductivity of pristine graphene, κ_0. An overall analysis exhibits a reduction of the thermal conductivity with increasing the pore size. Results demonstrate a change in the normalised thermal conductivity from 0.7 to 0.27 with increasing the void diameter from 2 nm to 6 nm at temperature of 100 K. This change in the thermal conductivity of defective graphene depends on the temperature for either chirality. For example, the normalised thermal conductivity of the zigzag graphene sheets with voids in a diameter of 2 nm raises from 0.7 to 0.84 through changing temperature from 100 K to 500 K, while this change for the armchair graphene is negligible for the temperature more than 300 K. Therefore, in addition to temperature, the pore size effect on the thermal conductivity depends on the chirality of graphene as well. Now let us compare those results with previous studies on atomic-scale defects, which are mainly missing atoms or bonding distortions distributed in the lattice structure of graphene observed through experimental examinations [48]. A reduction of the thermal conductivity of graphene about 75 % was reported in the presence of 1 % Stone-Wales or bivacancy defects [31, 32], which is comparable with the thermal conductivity of graphene sheets with a void in a diameter of 6 nm representing a defect density of 5.6%. A similar change in the thermal conductivity were reported for graphene with 3 % nitrogen atoms [33]. This indicates a severe impact on the thermal conductivity from induced atomic defects during fabrication

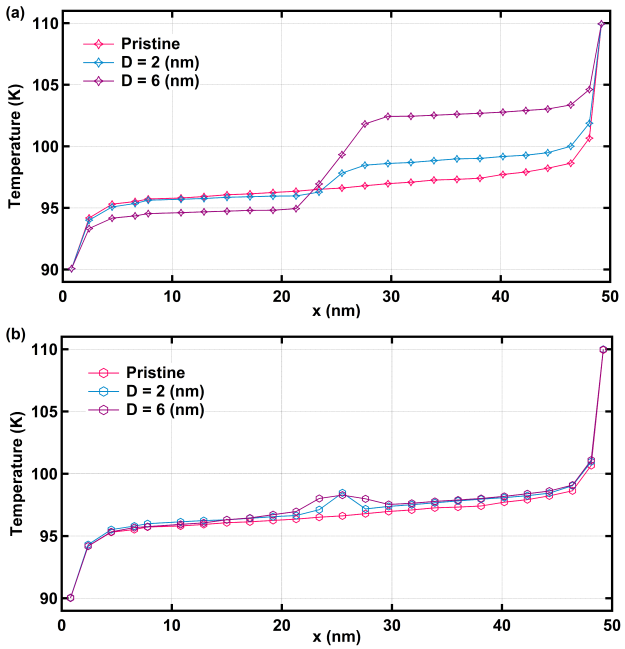

Figure 4: Temperature profile in a steady-state heat transfer at temperature of 100 K along the zigzag graphene sheets having (a) void and (b) bilayer defects with a diameter of D.

processes compared to nanoscale voids. The significant difference between atomic-scale defects and nanoscale ones on the thermal conductivity of graphene can be discussed through various aspects. The impact of defect distribution on the thermal transport parameters —including temperature gradient and heat flux (Eq. 1) —is one aspect to be considered. For example, the temperature gradient in defect regions is different than those with the prefect crystal structure of graphene. Atomic-scale defects are distributed along graphene sheets [30–32, 34], while, in contrast, nanoscale defects are constrained in one region as shown in Fig. 1. Therefore, distributed atomic-scale defects in graphene constitutes more changes along the thermal gradient compared to those nanoscale pinholes. The phonon transport is another aspect to be considered to explain the difference between atomic-scale defects and nanoscale ones on the thermal behaviour of graphene, which will be discussed in the following.

Now we proceed with the incorporation of bilayer defects on the thermal conductivity of graphene. In this study, atomic interactions in each graphene layer are modelled through using the optimised Tersoff potential [40], while Lennard-Jones [44] is used to model carbon interactions between graphene layers. The Lennard-Jones potential for interlayer interactions is found to be weak to model bilayer defects with a diameter of 2 nm at a temperature more than 100 K. The influence of bilayer defects on the thermal conductivity of the single layer graphene is analysed based on the defect size and temperature. First, the size effect is studied at temperature of 100 K (Fig. 6 (a)). The thermal conductivity of zigzag graphene reduces about 5 % with increasing the defect diameter to 4 nm. This change raises to 13 % for a bilayer defect with a diameter of 6 nm. For the armchair chirality, independent of the bilayer defect size, a reduction about 15 % is observed for the thermal transfer of graphene sheets. While, similar to voids (pinholes), bilayer defects reduce the thermal conductivity of graphene, the impact of bilayer defects on the thermal behaviour of graphene is significantly less than void defects (Fig. 5). After analysing the bilayer defect size, the effect of temperature on the thermal trasport is studied for graphene sheets having bilayer defects with a diameter of 6 nm (Fig. 6 (b)). In the first instance, results demonstrate that raising temperature reduces the impact of bilayer defects on the thermal behaviour of graphene for either chirality. A normalised thermal conductivity about 0.85 is obtained for defective graphene sheets at temperature of 100 K, while the thermal transport changes to about the thermal conductivity of defect-free graphene at temperature of 500 K. Although the

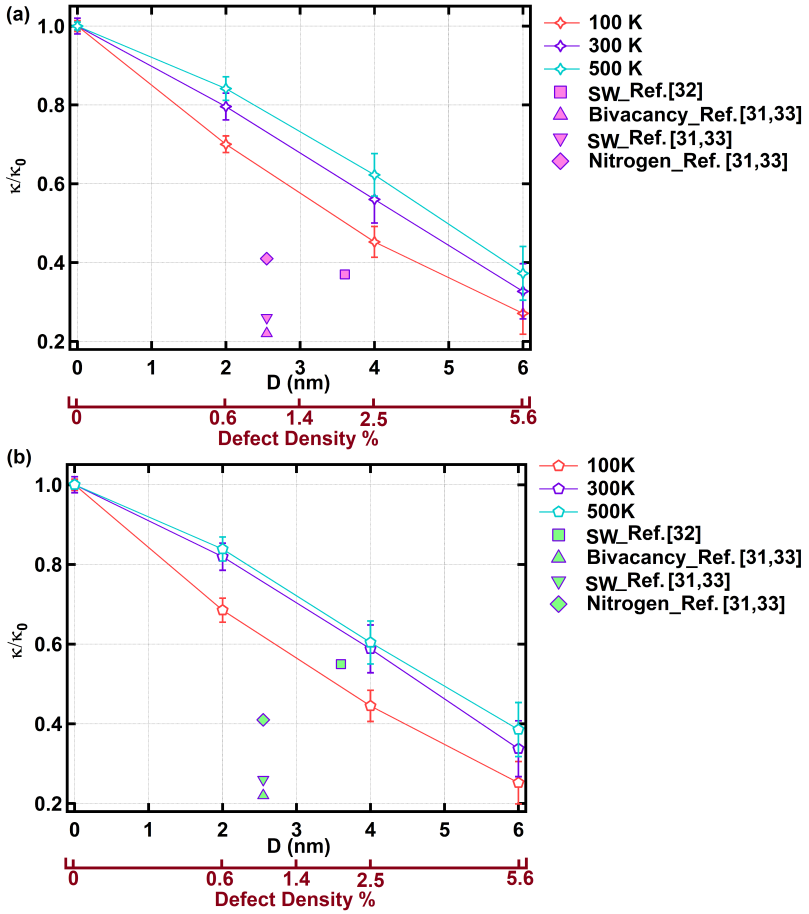

Figure 5: Normalised thermal conductivity of the (a) zigzag and (b) armchair graphene as a function of void size for temperature of 100 K to 500 K. Defect density for each diameter is indicated on an unscaled red axis. Results compared with atomic-scale defects including 2 % Stone-Wales (SW), 1 % Bivacancy and 1 % Nitrogen defects at temperature of 300 K from Ref. [31–33].

thermal behaviour of multi-layers graphene was studied previously [42], here, for the first time, the influence of bilayer defects on the thermal transfer of the single layer graphene is investigated as a function of size. Increasing temperature reduces the impact of bilayer defects on the thermal conductivity, where a similar behaviour has been obtained for void defects as well (Fig. 5). This temperature effect has been observed on the thermal behaviour of defective graphene sheets through previous studies, which is attributed to the dominance of phonon-defect scattering compared to phonon-phonon scattering [32, 43, 49].

The thermal conductivity of graphene with a perfect crystal structure is controlled by phonon-phonon scattering, known as intrinsic. Defects in graphene change the thermal transport through extrinsic effects of phonon-defect scattering [13]. One can compute the number of vibrational states per unit frequency, called density of state (DOS), to evaluate the phonon scattering in defective graphene, which is frequently used to explain the thermal conductivity of graphene with atomic-scale defects [30, 31, 33]. An overall analysis on the mechanism of thermal transfer in graphene sheets with void and bilayer defects can be obtained through phonon DOS computations. The phonon spectrum is calculated by Fourier transform of the velocity autocorrelation function during the steady-state condition [50] as

$$DOS(\omega) = \frac{1}{\sqrt{2\pi}} \int e^{-i\omega t} < v(t)v(0) > dt \tag{3}$$

Here ω is the frequency and v is the velocity of carbon atoms. Fig. 7 demonstrates DOS for defect-free

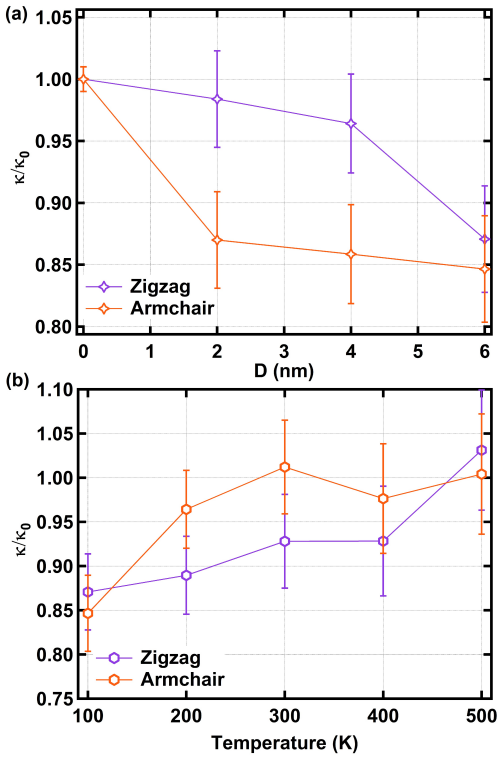

Figure 6: Normalised thermal conductivity of graphene sheets with bilayer defects (a) as a function of the bilayer defect size at temperature of 100 K, (b) with a diameter of 6 nm as function of temperature.

graphene and graphene sheets having void and bilayer defects with a diameter of 6 nm at temperature of 500 K. Those computations were performed for the zigzag chirality. The pristine graphene exhibits two main peaks at frequencies around 12 THz and 50 THz representing ballistic thermal transport. A similar spectrum is obtained for the graphene sheet with a bilayer defect. While DOS for both defect-free and bilayer defect graphene sheets are identical, low frequency peak is enhanced significantly at the graphene sheet with a void defect. This can be linked to the scattering of phonons through defects in graphene [20], which leads to the reduction of graphene thermal conductivity. Fig. 7 exhibits a slight damping about 12 % in the main peak at 50 THz in the graphene sheet with void defect. This damping of the main peak is reported to be significant due to atomic scale defects [31, 33]. Therefore, the severe effect of atomic defects compared to nanoscale ones (demonstrated in Fig. 5) on the graphene thermal conductivity can be linked to the intensity of phonon scattering. The insignificant change of the thermal conductivity in graphene sheets due to the presence of bilayer regions as observed in Fig. 6 can be traced backed to the low collision of phonons, similar to the ballistic thermal transport in defect-free graphene.

The influence of void and bilayer defects on the thermal behaviour of graphene has been discussed so far for circular shape, while nanoscale defects (voids and bilayer regions) with oval shapes have been observed during the fabrication processes [16, 24, 36, 37, 51]. Moreover, recent studies highlight the importance of pore shape on the physical behaviour of nanomaterials [52, 53]. Void and bilayer shape effects on the thermal conductivity of graphene are studied for elliptical profile. Here, NEMD method is used to model the thermal conductivity of graphene sheets with horizontal ellipse (H-ellipse) and vertical ellipse (V-ellipse) defects as shown in Fig. 8, where the defect density is the same as those with circular shape in a diameter of 6 nm. This leads to a defect density, defined as the density of defect over the density of defect-free graphene sheet, of 5.6 %. The H-ellipse and V-ellipse defect shapes stand for the major axis of the ellipse aligned and orthogonal to the heat flow direction (x-direction), respectively.

Fig. 9 exhibits the effect of void and bilayer shape on the thermal conductivity of graphene. An overall

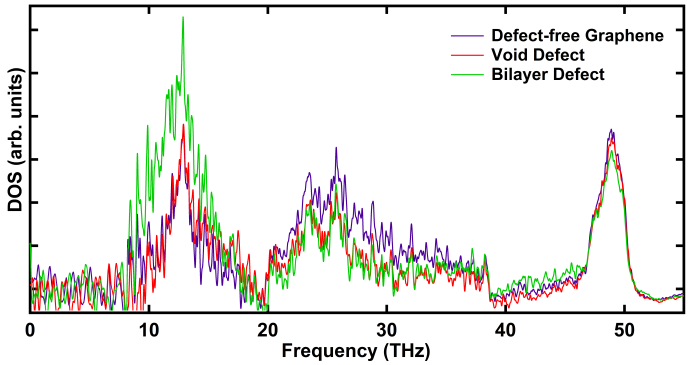

Figure 7: Phonon spectra of graphene sheets with (a) defect-free structure, (b) void and (c) bilayer defects in a diameter of 6 nm in the zigzag chirality at temperature of 500 K.

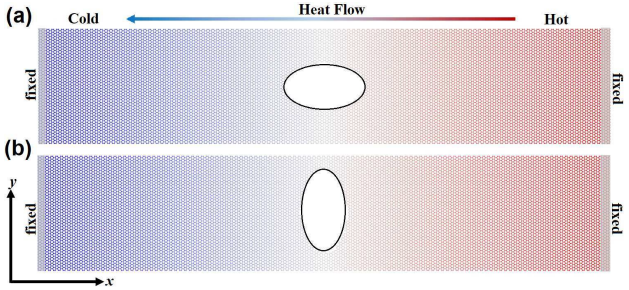

Figure 8: Schematic of NEMD model to calculate the thermal conductivity of single layer graphene with nanoscale (a) H-ellipse, and (b) V-ellipse defects with a defect density of 5.6 %.

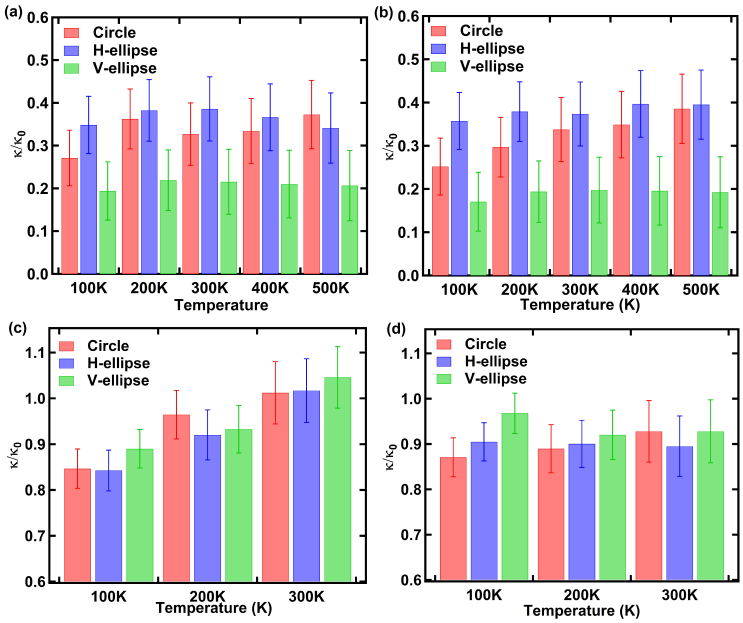

Figure 9: Normalised thermal conductivity as a function of temperature for the zigzag graphene with (a) void and (c) bilayer defects, and the armchair graphene with (b) void, (d) bilayer defects in different shapes of circle, H-ellipse and V-ellipse with the same defect density.

analysis demonstrates a significant defect shape effect on the thermal transfer. Starting from void defects, a lower thermal conductivity is obtained for the V-ellipse shape in either chirality, while the H-ellipse shape has the utmost thermal conductivity for both zigzag and armchair directions (Fig.9 (a) and (b)). The scenario of the defect shape is completely different for bilayer defects, where the V-ellipse shape exhibits a higher thermal conductivity compared to those with H-ellipse and circular shapes. A higher thermal conductivity in the H-ellipse pore shape compared to the V-ellipse and circle shapes was reported previously for defective graphene [34]. Defect shapes can be controlled during the fabrication processes to optimise the physical properties of graphene [24, 51, 54]. Although this work focus on the thermal transport in graphene with defects in circular and elliptical shapes based on experimental observations [16, 24, 36, 37, 51], studying other defect shapes remains for further investigations. Here a nanoscale defect in graphene sheets is modelled to study the thermal behaviour, while experimental observations have presented a range of nanoscale defects with various shapes distributed across graphene sheets [16, 21–24]. Multiscale modelling approaches can be used to model the thermal transfer of graphene sheets with randomly distributed defects through further studies [55].

4. Concluding remarks

This work addresses the impact of nanoscale void and bilayer defects on the thermal behaviour of graphene sheets. Here NEMD computations are used to study defect size effects on the zigzag and armchair oriented graphene. Although findings exhibit a reduction on the thermal conductivity of graphene sheets with increasing the defect size, the thermal transfer is more sensitive with voids compared to bilayer defects. The change in the thermal conductivity of defective graphene is found to be less through raising temperature due to the dominance of phonon-defect scattering compared to phonon-phonon scattering. Here results are compared with previously presented atomic-scale defects, which indicates a dramatic influence of atomic defects on the thermal conductivity compared to nanoscale voids due to a higher phonon scattering. This raises attention on the development of fabrication process more on atomic defects [16, 48]. After studying the defect size, this work investigates the influence of nanoscale defect shapes on the thermal behaviour of graphene, which demonstrates a significant defect shape effect with a higher thermal conductivity in elliptical shapes compared to circular ones with the same defect density. This can be linked to defect projected area perpendicular to the heat flow direction [34]. This study sheds light on defective graphene for engineering design in manufacturing process as well as multifunctional purposes.

References

[1] Y. Shao, J. Wang, H. Wu, J. Liu, I. A. Aksay, Y. Lin, Graphene based electrochemical sensors and biosensors: a review, Electroanalysis: An International Journal Devoted to Fundamental and Practical Aspects of Electroanalysis 22 (2010) 1027–1036.

[2] F. Schwierz, Graphene transistors, Nature nanotechnology 5 (2010) 487.

[3] M. Pumera, Graphene-based nanomaterials for energy storage, Energy & Environmental Science 4 (2011) 668–674.

[4] A. Manta, M. Gresil, C. Soutis, Tensile and flexural behaviour of a graphene/epoxy composite: experiments and simulation, Journal of Physics: Materials 3 (2019) 014006.

[5] M. Gresil, Z. Wang, Q.-A. Poutrel, C. Soutis, Thermal diffusivity mapping of graphene based polymer nanocomposites, Scientific Reports 7 (2017) 1–10.

[6] A. Manta, M. Gresil, C. Soutis, Predictive model of graphene based polymer nanocomposites: electrical performance, Applied Composite Materials 24 (2017) 281–300.

[7] A. K. Geim, K. S. Novoselov, The rise of graphene, in: Nanoscience and technology: a collection of reviews from nature journals, World Scientific, 2010, pp. 11–19.

[8] C. Lee, X. Wei, J. W. Kysar, J. Hone, Measurement of the elastic properties and intrinsic strength of monolayer graphene, science 321 (2008) 385–388.

[9] A. A. Balandin, S. Ghosh, W. Bao, I. Calizo, D. Teweldebrhan, F. Miao, C. N. Lau, Superior thermal conductivity of single-layer graphene, Nano letters 8 (2008) 902–907.

[10] D. Ghosh, I. Calizo, D. Teweldebrhan, E. P. Pokatilov, D. L. Nika, A. A. Balandin, W. Bao, F. Miao, C. N. Lau, Extremely high thermal conductivity of graphene: Prospects for thermal management applications in nanoelectronic circuits, Applied Physics Letters 92 (2008) 151911.

[11] P. Goli, S. Legedza, A. Dhar, R. Salgado, J. Renteria, A. A. Balandin, Graphene-enhanced hybrid phase change materials for thermal management of li-ion batteries, Journal of Power Sources 248 (2014) 37–43.

[12] J. Xiao, D. Mei, X. Li, W. Xu, D. Wang, G. L. Graff, W. D. Bennett, Z. Nie, L. V. Saraf, I. A. Aksay, et al., Hierarchically porous graphene as a lithium–air battery electrode, Nano letters 11 (2011) 5071–5078.
[13] A. A. Balandin, Thermal properties of graphene and nanostructured carbon materials, Nature materials 10 (2011) 569–581.
[14] C. Tang, B.-Q. Li, Q. Zhang, L. Zhu, H.-F. Wang, J.-L. Shi, F. Wei, Cao-templated growth of hierarchical porous graphene for high-power lithium–sulfur battery applications, Advanced Functional Materials 26 (2016) 577–585.
[15] A. Hashimoto, K. Suenaga, A. Gloter, K. Urita, S. Iijima, Direct evidence for atomic defects in graphene layers, Nature 430 (2004) 870–873.
[16] H. C. Lee, W.-W. Liu, S.-P. Chai, A. R. Mohamed, A. Aziz, C.-S. Khe, N. M. Hidayah, U. Hashim, Review of the synthesis, transfer, characterization and growth mechanisms of single and multilayer graphene, RSC advances 7 (2017) 15644–15693.
[17] A. Manta, M. Gresil, C. Soutis, Infrared thermography for void mapping of a graphene/epoxy composite and its full-field thermal simulation, Fatigue & Fracture of Engineering Materials & Structures 42 (2019) 1441–1453.
[18] J. H. Seol, I. Jo, A. L. Moore, L. Lindsay, Z. H. Aitken, M. T. Pettes, X. Li, Z. Yao, R. Huang, D. Broido, et al., Two-dimensional phonon transport in supported graphene, Science 328 (2010) 213–216.
[19] M. M. Sadeghi, M. T. Pettes, L. Shi, Thermal transport in graphene, Solid State Communications 152 (2012) 1321–1330.
[20] F. Banhart, J. Kotakoski, A. V. Krasheninnikov, Structural defects in graphene, ACS nano 5 (2011) 26–41.
[21] S. C. O'Hern, C. A. Stewart, M. S. Boutilier, J.-C. Idrobo, S. Bhaviripudi, S. K. Das, J. Kong, T. Laoui, M. Atieh, R. Karnik, Selective molecular transport through intrinsic defects in a single layer of cvd graphene, ACS nano 6 (2012) 10130–10138.
[22] Ç. Ö. Girit, J. C. Meyer, R. Erni, M. D. Rossell, C. Kisielowski, L. Yang, C.-H. Park, M. Crommie, M. L. Cohen, S. G. Louie, et al., Graphene at the edge: stability and dynamics, science 323 (2009) 1705–1708.
[23] G. Compagnini, F. Giannazzo, S. Sonde, V. Raineri, E. Rimini, Ion irradiation and defect formation in single layer graphene, Carbon 47 (2009) 3201–3207.
[24] N. Lu, J. Wang, H. C. Floresca, M. J. Kim, In situ studies on the shrinkage and expansion of graphene nanopores under electron beam irradiation at temperatures in the range of 400–1200 c, Carbon 50 (2012) 2961–2965.
[25] C. A. Merchant, K. Healy, M. Wanunu, V. Ray, N. Peterman, J. Bartel, M. D. Fischbein, K. Venta, Z. Luo, A. C. Johnson, et al., Dna translocation through graphene nanopores, Nano letters 10 (2010) 2915–2921.
[26] H. Malekpour, P. Ramnani, S. Srinivasan, G. Balasubramanian, D. L. Nika, A. Mulchandani, R. K. Lake, A. A. Balandin, Thermal conductivity of graphene with defects induced by electron beam irradiation, Nanoscale 8 (2016) 14608–14616.
[27] J. Hu, X. Ruan, Y. P. Chen, Thermal conductivity and thermal rectification in graphene nanoribbons: a molecular dynamics study, Nano letters 9 (2009) 2730–2735.
[28] Z. Guo, D. Zhang, X.-G. Gong, Thermal conductivity of graphene nanoribbons, Applied physics letters 95 (2009) 163103.
[29] X. Wang, X. Wang, Z. Wang, Y. Guo, Y. Wang, Enhancing mechanism of interfacial metal element on the thermal transport across cu-graphene interfaces revealed by molecular dynamics simulations, Materials Today Communications (2020) 101431.
[30] Y. Wang, S. Chen, X. Ruan, Tunable thermal rectification in graphene nanoribbons through defect engineering: A molecular dynamics study, Applied Physics Letters 100 (2012) 163101.
[31] B. Mortazavi, S. Ahzi, Thermal conductivity and tensile response of defective graphene: A molecular dynamics study, Carbon 63 (2013) 460–470.
[32] T. Y. Ng, J. J. Yeo, Z. Liu, A molecular dynamics study of the thermal conductivity of graphene nanoribbons containing dispersed stone–thrower–wales defects, Carbon 50 (2012) 4887–4893.
[33] B. Mortazavi, A. Rajabpour, S. Ahzi, Y. Rémond, S. M. V. Allaei, Nitrogen doping and curvature effects on thermal conductivity of graphene: A non-equilibrium molecular dynamics study, Solid state communications 152 (2012) 261–264.
[34] N. Zhan, B. Chen, C. Li, P. K. Shen, Molecular dynamics simulations of the thermal conductivity of graphene for application in wearable devices, Nanotechnology 30 (2018) 025705.
[35] M. Nasr Esfahani, B. E. Alaca, A review on size-dependent mechanical properties of nanowires, Advanced Engineering Materials 21 (2019) 1900192.
[36] M. Kruskopf, R. E. Elmquist, Epitaxial graphene for quantum resistance metrology, Metrologia 55 (2018) R27.
[37] N. Srivastava, G. He, R. M. Feenstra, P. Fisher, et al., Comparison of graphene formation on c-face and si-face sic {0001} surfaces, Physical Review B 82 (2010) 235406.
[38] B. Premlal, M. Cranney, F. Vonau, D. Aubel, D. Casterman, M. De Souza, L. Simon, Surface intercalation of gold underneath a graphene monolayer on sic (0001) studied by scanning tunneling microscopy and spectroscopy, Applied Physics Letters 94 (2009) 263115.
[39] S. Rajput, Y. Li, L. Li, Direct experimental evidence for the reversal of carrier type upon hydrogen intercalation in epitaxial graphene/sic (0001), Applied Physics Letters 104 (2014) 041908.
[40] L. Lindsay, D. Broido, Optimized tersoff and brenner empirical potential parameters for lattice dynamics and phonon thermal transport in carbon nanotubes and graphene, Physical Review B 81 (2010) 205441.
[41] S. Plimpton, Fast parallel algorithms for short-range molecular dynamics, Technical Report, Sandia National Labs., Albuquerque, NM (United States), 1993.
[42] H.-Y. Cao, Z.-X. Guo, H. Xiang, X.-G. Gong, Layer and size dependence of thermal conductivity in multilayer graphene nanoribbons, Physics Letters A 376 (2012) 525–528.
[43] Y.-Y. Zhang, Y. Cheng, Q.-X. Pei, C. Wang, Y. Xiang, Thermal conductivity of defective graphene, Physics Letters A 376 (2012) 3668–3672.
[44] L. Girifalco, M. Hodak, R. S. Lee, Carbon nanotubes, buckyballs, ropes, and a universal graphitic potential, Physical Review B 62 (2000) 13104.

[45] Z. Fan, L. F. C. Pereira, H.-Q. Wang, J.-C. Zheng, D. Donadio, A. Harju, Force and heat current formulas for many-body potentials in molecular dynamics simulations with applications to thermal conductivity calculations, Physical Review B 92 (2015) 094301.
[46] G. Fugallo, A. Cepellotti, L. Paulatto, M. Lazzeri, N. Marzari, F. Mauri, Thermal conductivity of graphene and graphite: collective excitations and mean free paths, Nano letters 14 (2014) 6109–6114.
[47] Y. Hu, T. Feng, X. Gu, Z. Fan, X. Wang, M. Lundstrom, S. S. Shrestha, H. Bao, Unification of nonequilibrium molecular dynamics and the mode-resolved phonon boltzmann equation for thermal transport simulations, Physical Review B 101 (2020) 155308.
[48] L. Vicarelli, S. J. Heerema, C. Dekker, H. W. Zandbergen, Controlling defects in graphene for optimizing the electrical properties of graphene nanodevices, ACS nano 9 (2015) 3428–3435.
[49] T.-H. Fang, Z.-W. Lee, W.-J. Chang, C.-C. Huang, Determining porosity effect on the thermal conductivity of single-layer graphene using a molecular dynamics simulation, Physica E: Low-dimensional Systems and Nanostructures 106 (2019) 90–94.
[50] G. Grest, S. Nagel, A. Rahman, T. Witten Jr, Density of states and the velocity autocorrelation function derived from quench studies, The Journal of Chemical Physics 74 (1981) 3532–3534.
[51] H. Vázquez, E. Åhlgren, O. Ochedowski, A. Leino, R. Mirzayev, R. Kozubek, H. Lebius, M. Karlušic, M. Jakšic, A. Krasheninnikov, et al., Creating nanoporous graphene with swift heavy ions, Carbon 114 (2017) 511–518.
[52] M. Nasr Esfahani, M. Jabbari, Molecular dynamics simulations of deformation mechanisms in the mechanical response of nanoporous gold, Materials 13 (2020) 2071.
[53] M. N. Esfahani, B. E. Alaca, M. Jabbari, Mechanical properties of honeycomb nanoporous silicon: a high strength and ductile structure, Nanotechnology 30 (2019) 455702.
[54] Z. Bai, L. Zhang, H. Li, L. Liu, Nanopore creation in graphene by ion beam irradiation: geometry, quality, and efficiency, ACS applied materials & interfaces 8 (2016) 24803–24809.
[55] A. Manta, M. Gresil, C. Soutis, Simulated electrical response of randomly distributed and aligned graphene/polymer nanocomposites, Composite Structures 192 (2018) 452–459.